

Movement Dynamics in Elite Female Soccer Athletes: The Quantile Cube Approach

Kendall L. Thomas¹ and Jan Hannig¹

¹Department of Statistics and Operations Research, University of North
Carolina at Chapel Hill, Chapel Hill, NC, US

Abstract

This paper presents an innovative adaptation of existing methodology to investigate external load in elite female soccer athletes using GPS-derived movement data from 23 matches. We developed a quantitative framework to examine velocity, acceleration, and movement angle across game halves, enabling transparent and meaningful performance insights. By constructing a quantile cube to quantify movement patterns, we segmented athletes' movements into distinct velocity, acceleration, and angle quantiles. Statistical analysis revealed significant differences in movement distributions between match halves for individual athletes. Principal Component Analysis (PCA) identified anomalous games with unique movement dynamics, particularly at the start and end of the season. Dirichlet-multinomial regression further explored how factors like athlete position, playing time, and game characteristics influenced movement profiles. This approach provides a structured method for analyzing movement dynamics, revealing external load variations over time and offering insights into performance optimization. The integration of these statistical techniques demonstrates the potential of data-driven strategies to enhance athlete monitoring in soccer.

Keywords: Dirichlet-multinomial regression; Principal Component Analysis; Hellinger distance; multivariate analysis; GPS tracking

1 Introduction

The increasing use of wearable technology in sports has transformed how athletic performance is monitored and analyzed, especially among elite athletes. These technologies generate vast quantities of data that provide a deeper understanding of the demands placed on athletes, enabling more precise adjustments to training regimens (Cummins et al., 2013). The integration of advanced data analytics with wearable technology has become essential in extracting actionable insights from these datasets, particularly when evaluating training volume and intensity (Bourdon et al., 2017). A key component of this is external load monitoring using global positioning system (GPS) technology, which has gained widespread adoption for quantifying movement patterns and load metrics. While these devices provide valuable data for making data-driven decisions regarding training programs and performance optimization, significant challenges exist in interpreting and standardizing their outputs. Many wearable device companies provide proprietary “training load” metrics that integrate multiple factors—including session duration, distance covered, speed thresholds, and acceleration events—but the exact formulas and component definitions remain undisclosed and vary across manufacturers. This lack of transparency raises important questions about the consistency and comparability of metrics across different devices and their utility in making reliable, actionable decisions.

Research has explored statistical inference techniques for longitudinal data, such as GPS-derived metrics, to address the computational challenges posed by a continuously expanding dataset. Historically, research in this space is based on the assumptions of independent and identically distributed data, which is not upheld in the real-world (Luo and Song, 2020). Recent studies, however, have begun to explore methods that do not make this assumption with the use of techniques such as linear state-space mixed models and incremental inference via dynamic updates (Luo and Song, 2023; Luo et al., 2023). For example, Luo et al. (2023) propose an innovative framework that leverages the summation of summary statistics over data batches, enabling dynamic updates to point estimates and standard errors. However, while such methods streamline analysis,

relying on summary statistics may obscure important changes at the extremes of the data distribution, which are often critical for identifying actionable insights and capturing nuanced patterns in longitudinal data. To address these limitations and extract more comprehensive insights from the expanding datasets, researchers have increasingly turned to more sophisticated approaches that combine multiple data sources.

Building on these foundational statistical approaches, the integration of advanced data analytics with wearable technology has become essential for extracting actionable insights from these datasets, particularly when evaluating training volume, intensity, and fatigue patterns (Bourdon et al., 2017). Emerging studies demonstrate the value of combining GPS-derived external load metrics with advanced machine learning approaches to enhance injury prediction. For instance, Vallance et al. (2020) demonstrate how integrating internal (e.g., subjective well-being) and external (e.g., GPS-derived metrics) training loads for professional male soccer players can improve injury forecasting using non-linear models. Similarly, Rossi et al. (2018) highlight the benefits of multi-dimensional frameworks for understanding relationships between training load patterns and injury risk. These integrated approaches demonstrate promising results in male professional sports, though their implementation and validation across diverse athletic populations remain areas for further investigation.

However, significant challenges persist in the practical application of these technologies. While machine learning models have shown promise in injury prediction, their complexity often makes them less accessible for coaching and training staff. As Ferraz et al. (2023) emphasize in their work, there is a pressing need for integrative models that combine external load data with internal load metrics in team sports. The absence of such unified analytical frameworks limits the ability to fully leverage these datasets for actionable insights, particularly in women's sports, where limited research further complicates the issue. This research gap highlights the urgent need for the development of analytical frameworks that are not only interpretable but also practical for real-time application.

This paper seeks to address these gaps by proposing a novel method for integrating

GPS-based external load monitoring with athlete and match characteristics in elite female soccer athletes. Our primary objective is to quantify movement patterns, focusing specifically on velocity, acceleration, and angle of movement during match play, and to explore their relationships with athlete performance and match outcomes. We introduce an innovative adaptation of existing methodologies that combines statistical transparency with probabilistic modeling, offering a structured, interpretable approach to quantifying movement patterns and exploring their relationships with athlete traits. This research aims to bridge the gap between data collection and practical application by establishing a data-driven foundation for optimizing training protocols, leveraging statistical inference to quantify the relationship between movement patterns and athlete workload.

The paper is organized as follows: Section 2 details the data and proposed summaries to be used in downstream analysis, Section 3 presents our methods and results, and Section 4 concludes our work and provides a discussion on the implications.

2 Data

The data was collected by the Applied Physiology Lab in the Exercise Science Department at UNC Chapel Hill and shared under IRB 23-2673.

We obtained GPS data from all match sessions over one season for 33 elite female soccer athletes. For the initial investigation, we selected athletes who played consistently high minutes (> 25 min per half) in over five match sessions, resulting in nine athletes. By this criterion, we used a total of 23 matches between nine athletes for our analysis. The raw data contains one data point of a longitude and latitude coordinate per second for the time played in the match as shown on the left in Figure 1 (Google Maps API, 2025). For example, if the athlete played 80 minutes of a match session, the raw data from the wearable device contained 4800 rows of data, each with a timestamp, longitude, and latitude coordinate for the athlete's location.

In order to calculate velocity, acceleration, and angle of movement from the raw data, we first converted the longitude and latitude coordinates to an (x, y) coordinate representing the location in meters (Pebesma, 2018). We then fit a third-degree interpolating

spline to the data, using ten points per second, to model the movements of the athlete as shown on the right in Figure 1. From the spline representation, we calculated the velocity (m/s) and acceleration (m/s^2) through the first and second derivatives, respectively. We then computed the angle of movement as modulo 360 of the difference between the velocity angle and acceleration angle. Lastly, we shifted the angle to range between -180 and 180 degrees to enhance directional interpretability. We thresholded any velocity values less than 0.01 or acceleration values less than 0.001 to 0, and used a transformation of $\log_{10}(1 + \text{velocity})$ and $\log_{10}(1 + \text{acceleration})$ for easier interpretation, since the raw data was heavily skewed right.

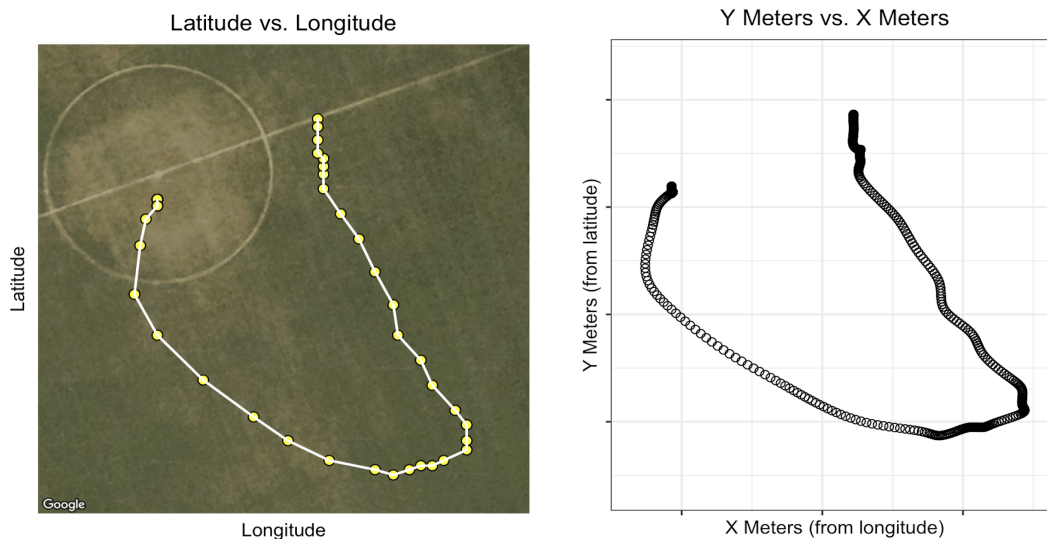


Figure 1: Left: Raw GPS data for 50 seconds of movement for one athlete overlaid on a satellite map (source: (Google Maps API, 2025)). Right: Interpolating Spline in meters fit to the same 50 seconds of movement for one athlete seen on the left. Note, for confidentiality purposes, longitude and latitude coordinates and converted meters are not displayed.

Note, from here we refer to $\log_{10}(1 + \text{velocity})$ and $\log_{10}(1 + \text{acceleration})$ as just velocity and acceleration, respectively.

2.1 Quantile Cube

Understanding the distribution of movement characteristics such as velocity, acceleration, and angle is crucial for analyzing athlete performance and identifying patterns across different phases of a match. However, raw data alone can be noisy and difficult to

interpret, especially when comparing multiple athletes across various match sessions. To address this, we constructed a quantile cube to systematically capture and summarize the range of these movement variables. By discretizing the data into quantiles, we could better understand the time spent in certain types of movement patterns and detect trends within and between athletes.

In order to form the quantile cube, we used the spline representation of the data containing velocity, acceleration, and angle of movement at ten points per second for athletes who played at least 25 minutes in both halves of the game. We aggregated the data from all nine athletes across 23 match sessions to establish the quantile boundaries. For velocity and acceleration, we fit five quantiles (0-20th, 20-40th, 40-60th, 60-80th, and 80-100th percentiles) to determine the distribution bounds across the dataset. For angle of movement, we fit four quantiles, starting from a shifted baseline of -30 degrees, representing four primary directions of movement: forward, right, backward, and left. These values are displayed in Tables 1 and 2.

Quantile (%)	0%	20%	40%	60%	80%	100%
log(1 + velocity)	0.0043	0.1235	0.2789	0.3984	0.5561	1.0426
log(1+ acceleration)	0.0000	0.1529	0.2591	0.3604	0.4824	1.318

Table 1: Five quantiles for $\log(1 + \text{velocity})$ and $\log(1 + \text{acceleration})$

Quantile (%)	0%	25%	50%	75%	100%
Angle	-30.0000	31.6302	149.2631	-148.7042	-30.0000

Table 2: Four quantiles for angle, starting from a shifted baseline of -30 degrees

Using the established quantile boundaries, we constructed a quantile cube for each half of every game for each athlete, where each dimension of the cube represents one of the key metrics: velocity, acceleration, and angle of movement. The quantile cube can then be visually represented as in Figure 2 and Figure 3.

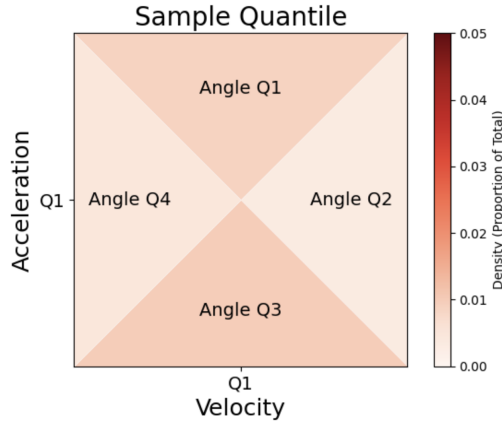


Figure 2: Legend for the visual representation of the quantile cube showing just the lower left quantile of the first half in Figure 3

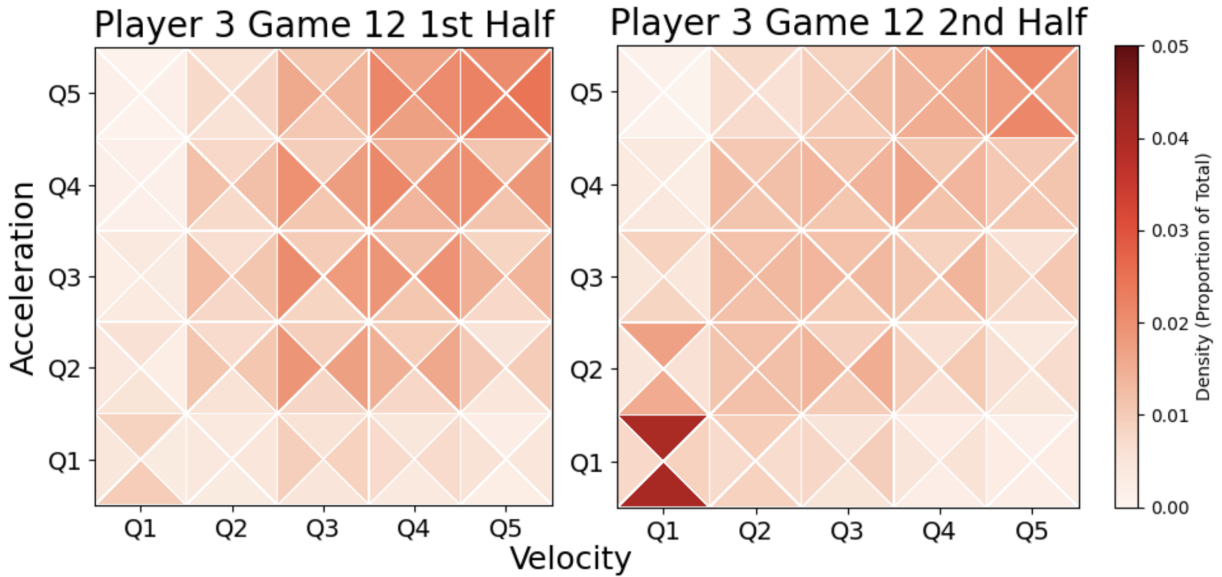


Figure 3: Visual representation of the quantile cube for the density of movements in the first half (left) and second half (right) of game 12 for player 3

The quantile cube can be represented either through raw counts (in deciseconds) or as proportions of total time spent in each segment. The proportions capture the athlete’s movement distribution across the velocity-acceleration-angle space. We summarize the data into a $n \times d$ matrix \mathbf{Y} where each of the $n = 396$ rows is a vectorized quantile cube of $d = 100$ dimension where each entry in the row represents the time spent in deciseconds in the corresponding movement quantile.

2.2 Covariates

In addition to the GPS data, we obtained certain covariates associated with each match and athlete, forming a matrix \mathbf{X} with $n = 396$ rows and $p = 13$ covariates. Match characteristics included the match ID, the location (home or away), half (1st or 2nd), result (win, loss, or tie), goals scored at both the end of the match and halftime, goals conceded at both the end of the match and halftime, and score differential at both the end of the match and halftime. Athlete characteristics included the athlete ID, position and playing time by half.

3 Methods and Results

3.1 Distributional Comparisons

Classically, several existing parametric methodologies are available to measure differences in distributions or means, both in general and over time. Simple approaches to testing for differences in means between two samples include the T-Test, ANOVA, and Hotelling's T^2 . However, these tests assume certain conditions, such as common variance, independence, and multivariate normality, which are not satisfied by our data (Casella and Berger, 2002). Moreover, focusing solely on the change point in the mean overlooks the complete range of fluctuations contributing to external load, neglecting extreme values that may be the primary drivers of change.

To address these limitations, the field has seen significant advancements in statistical methods tailored to high-dimensional data, where the number of variables p exceeds the sample size n . The work of Bai and Saranadasa (1996) introduces a high-dimensional two-sample test that adjusts for the breakdown of classical methods under such conditions by leveraging asymptotic properties of high-dimensional data when p and n are of the same order. Similarly, Chen and Qin (2010) developed a two-sample test specifically designed for high-dimensional applications such as gene-set testing, where p can be arbitrarily large and independent of n , provided a covariance condition is satisfied. These methods are innovative in their ability to handle scenarios where traditional assumptions

fail, particularly in cases of extreme dimensionality. However, these approaches often emphasize aggregate changes, such as shifts in mean or covariance, while neglecting extreme fluctuations that may drive critical changes in external load. By examining these foundational works, we highlight the necessity of alternative methodologies that can operate effectively in moderate-dimensional settings and incorporate the influence of extreme values into change-point detection frameworks.

We propose the use of Hellinger distance in this setting because our data can be viewed as multinomial samples (Vaart, 1998, pp.211-212). Recall that we have the observed count matrix $\mathbf{Y} = (y_{ij})_{n \times d}$ representing the quantile cubes and design matrix of covariates $\mathbf{X} = (x_{ik})_{n \times p}$. Thus, for each observation \mathbf{y}_i , we have a corresponding vector \mathbf{x}_i , including covariates of athlete ID, match ID, half, and playing time. For a given observation i , the variable $h_i \in \{1, 2\}$ indicates the half, where $h_i = 1$ indicates the first half and $h_i = 2$ indicates the second half. The match ID is denoted by $m_i \in \{1, \dots, 23\}$, and the athlete ID is denoted by $a_i \in \{1, \dots, 9\}$. Additionally, playing time, t_i , represents the athlete's playing time in deciseconds.

Let $P_{a,m}$ denote the underlying probability distribution of the quantile cube for athlete a in match m . For a fixed athlete a and match m , let $\hat{p}_{a,m,1}$ and $\hat{p}_{a,m,2}$ be the estimated probability vectors for the first and second halves, respectively. Then $P_{a,m}^{(1)}$ and $P_{a,m}^{(2)}$ correspond to the distributions for the first and second halves. Thus, we define our hypotheses as follows: the null hypothesis (\mathbf{H}_0) states that the distributions of the quantile cubes in the first and second halves follow the same underlying distribution, i.e., $H_0 : \hat{p}_{a,m,1} \sim P_{a,m}^{(1)}, \hat{p}_{a,m,2} \sim P_{a,m}^{(2)}$ with $P_{a,m}^{(1)} = P_{a,m}^{(2)}$. Conversely, the alternative hypothesis (\mathbf{H}_1) states that the underlying distributions differ, i.e., $H_1 : \hat{p}_{a,m,1} \sim P_{a,m}^{(1)}, \hat{p}_{a,m,2} \sim P_{a,m}^{(2)}$ with $P_{a,m}^{(1)} \neq P_{a,m}^{(2)}$.

To formally test this hypothesis, we used a Hellinger distance-based resampling test to quantify distributional differences between the multinomial count estimates of the first half and the second half. We chose the Hellinger distance over similar distance metrics, such as the Kullback-Leibler divergence, because it is symmetric and bounded. To form the null distribution, $P_{a,m}$, we performed a Monte Carlo simulation. That is,

for a fixed athlete a and match m with a corresponding covariate vector for the first half \mathbf{x}_1 , we randomly sampled t_1 counts with probabilities following the proportional representation of a quantile cube generated from the full dataset to represent a simulated first half. Similarly, with a corresponding covariate vector \mathbf{x}_2 for the second half, we randomly sampled t_2 counts with probabilities following the proportional representation of a quantile cube generated from the full dataset to represent a simulated second half. From these samples, we calculated $\hat{p}_{a,m,1}$ and $\hat{p}_{a,m,2}$ and their Hellinger distance under the null hypothesis: $l_1^i = H(\hat{p}_{a,m,1}, \hat{p}_{a,m,2})$. We repeated this process 10,000 times, starting with resampling, to form our null distributions: $P_{a,m} = (l_1^i, \dots, l_{1000}^i)$.

For the actual test statistic, we calculated the Hellinger distance between the first and second half count distributions for each match. For each athlete a and match m , we computed $\lambda_{a,m} = H(\hat{p}_{a,m,1}, \hat{p}_{a,m,2})$. We then performed a multiple comparison test using Bonferroni-corrected p-values at significance level $\hat{\alpha} = 0.05/g$, where g is the number of matches played by athlete a . Hence, we found the $(1 - \hat{\alpha})^{th}$ percentile $p_{P_{a,m}}$ such that $\mathbb{P}_{P_{a,m}}(H(\hat{p}_{a,m,1}, \hat{p}_{a,m,2}) > p_{P_{a,m}}) = \hat{\alpha}$.

The actual Hellinger distance values for each match were compared against the $(1 - \hat{\alpha})^{th}$ percentile of the null distribution, as shown in Figure 4 for Athlete 5. Specifically, the results, shown in Figure 5, demonstrate that for all athletes $a \in \{1, \dots, 9\}$ and matches $m \in \{1, \dots, 23\}$, the actual Hellinger distance values $\lambda_{a,m}$ exceed the null distribution thresholds $p_{P_{a,m}}$. Therefore, we reject the null hypothesis of identical movement distributions between halves at significance level $\hat{\alpha}$ for each athlete across all matches, concluding that $P_{a,m}^{(1)} \neq P_{a,m}^{(2)}$ for all a and m . We find a statistically significant difference in movement distribution between the two halves across all matches for all athletes.

Hellinger Distance vs. Game Date: Athlete 5

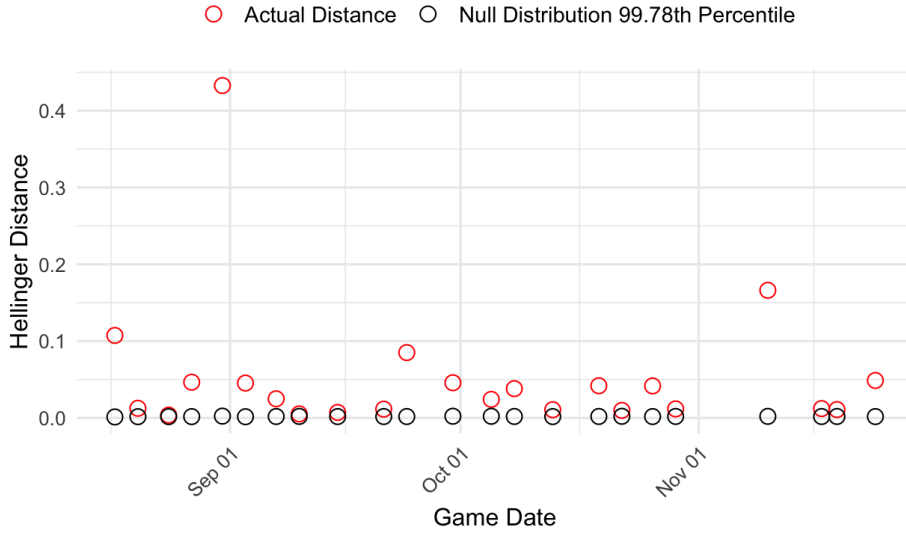


Figure 4: Hellinger distance by game date between the first and second halves for the actual game data (red circles) and the null distribution at the 99.78th percentile (black circles) for athlete 5. The red circles (actual distances) exceeded the black circles (null distribution) for all 23 games, indicating that the distributions of movements in the first and second halves are derived from different underlying distributions.

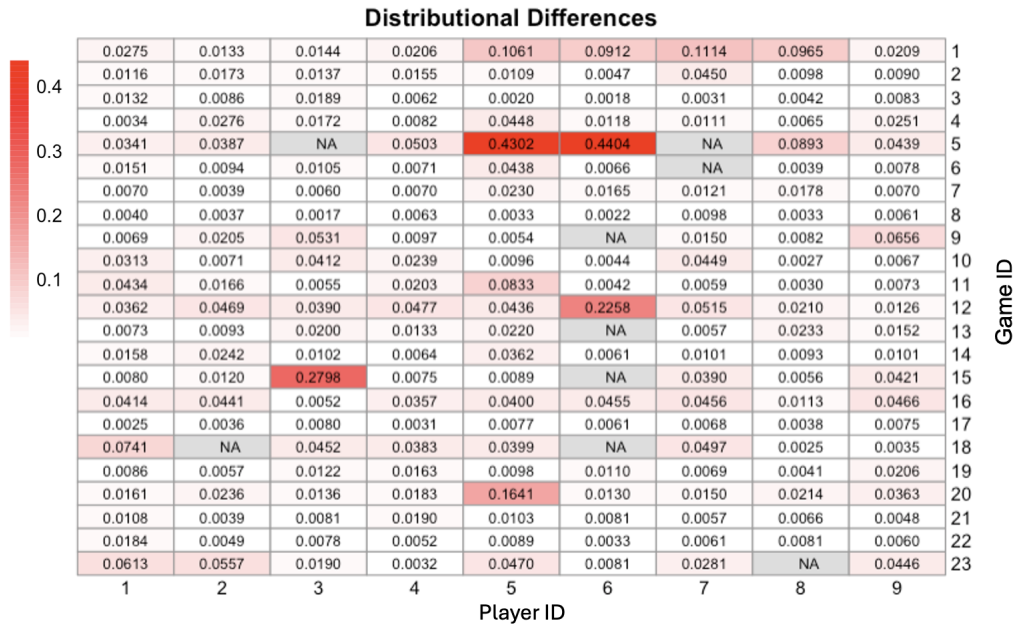


Figure 5: Heatmap showing the difference between the Hellinger distance for actual game data and the null distribution at the $\hat{\alpha}^{th}$ percentile for all athletes across all games. NA indicates that the athlete’s playing time did not meet the selection criteria for the game ID. Larger values (darker red) represent cases where the Hellinger distance for the actual game data exceeded the null distribution at the $\hat{\alpha}^{th}$ percentile.

3.2 Principal Component Analysis

To identify key patterns and reduce dimensionality in the dataset, Principal Component Analysis (PCA) was applied to the observed count matrix \mathbf{Y} representing the quantile cubes (Jolliffe, 2002). We aimed to capture dominant modes of variation in athlete movements across all matches in order to provide insight into anomalous patterns. This procedure resulted in $d = 100$ principal components (PCs), each with a corresponding $n = 396$ dimensional score. A cutoff of 90% variation was used to subset the top PCs, resulting in the retention of the first seven PCs. The first few components explained the majority of the variance, with a sharp drop in the explained variance ratio after the seventh component, justifying the focus on these seven PCs. To investigate clustering, the top components were plotted against one another and colored by covariates from the design matrix \mathbf{X} . Notably, PC1 and PC4 stood out as they capture specific and interpretable patterns related to key matches during the season.

PC1, which accounts for the largest proportion of variance, emphasizes distinct characteristics observed during the second half of the first game of the season. Specifically, it captures a reduced proportion of time spent in the middle quantiles of both velocity and acceleration, suggesting a potential shift in movement dynamics during that period. Table 3 lists the top 10 loadings by absolute value for PC1, where the highest loadings are associated with features combining the third velocity quantile and the fourth acceleration quantile with the third and first quantiles of angle. These features predominantly correspond to mid-range velocity and acceleration, particularly in the forward and backward directions. Furthermore, a histogram comparing the PC1 scores for all games with the scores from game 1, shown in Figure 6, reveals a clear deviation, confirming the unique nature of the second half of the first game.

PC4 captures unique characteristics of game 23, a season-ending loss. The top loadings by absolute value for PC4, shown in Table 4, are dominated by features that reflect low velocities combined with high acceleration. Notably, the highest loadings are associated with the first velocity quantile and the fifth acceleration quantile with the first and third quantiles of angle. This suggests a shift toward more intense, short-burst movements

during this critical match. The histogram in Figure 7 compares the PC4 scores for all games to game 23, highlighting the distinct movement pattern observed during the final game.

	Variable	PC1 Loading		Variable	PC4 Loading
1	Q3_vel_Q4_acc_Q3_angle	-0.1306	1	Q1_vel_Q5_acc_Q1_angle	0.3297
2	Q3_vel_Q4_acc_Q1_angle	-0.1300	2	Q1_vel_Q5_acc_Q3_angle	0.3179
3	Q4_vel_Q3_acc_Q3_angle	-0.1293	3	Q2_vel_Q5_acc_Q1_angle	0.2215
4	Q4_vel_Q3_acc_Q1_angle	-0.1290	4	Q2_vel_Q5_acc_Q3_angle	0.2111
5	Q4_vel_Q4_acc_Q1_angle	-0.1273	5	Q1_vel_Q5_acc_Q4_angle	0.2053
6	Q4_vel_Q4_acc_Q3_angle	-0.1271	6	Q1_vel_Q5_acc_Q2_angle	0.2022
7	Q4_vel_Q2_acc_Q4_angle	-0.1253	7	Q4_vel_Q5_acc_Q3_angle	0.1734
8	Q4_vel_Q2_acc_Q1_angle	-0.1253	8	Q3_vel_Q5_acc_Q3_angle	0.1709
9	Q2_vel_Q5_acc_Q2_angle	-0.1253	9	Q3_vel_Q5_acc_Q1_angle	0.1692
10	Q3_vel_Q3_acc_Q3_angle	-0.1253	10	Q4_vel_Q5_acc_Q1_angle	0.1642

Table 3: Top 10 PCA loadings by absolute value for PC1

Table 4: Top 10 PCA loadings by absolute value for PC4

Overall, PCA successfully reduced the dimensionality of the dataset while preserving the key patterns of variation across matches. PC1 and PC4 provided interpretable insights into specific matches, revealing differences in movement strategies during certain moments of the season.

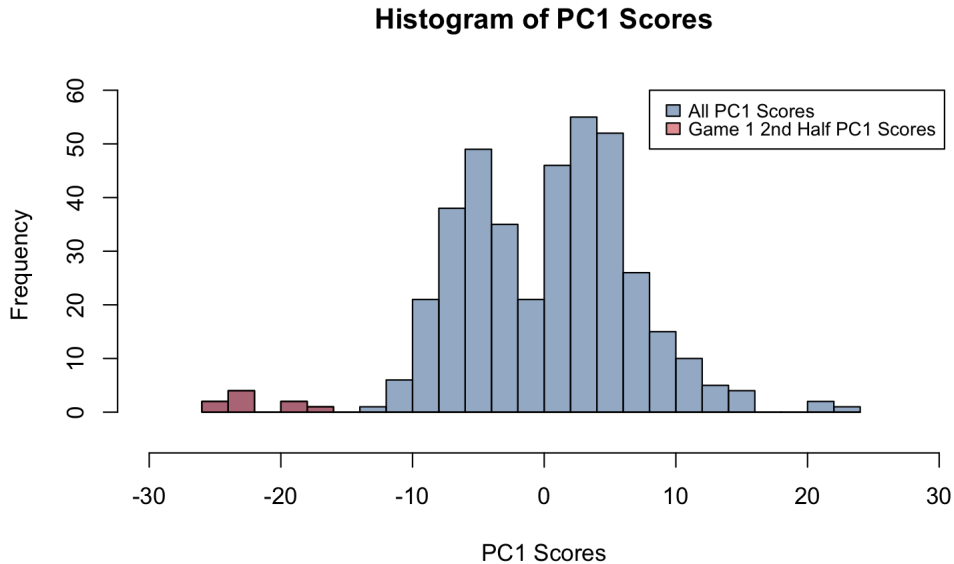


Figure 6: Histogram comparing the distribution of PC1 scores for all data (blue) versus the second half of Game 1 (red). The scores from the second half of Game 1 are more negative than the overall distribution, indicating a difference in underlying movement patterns in the corresponding quantiles during this period.

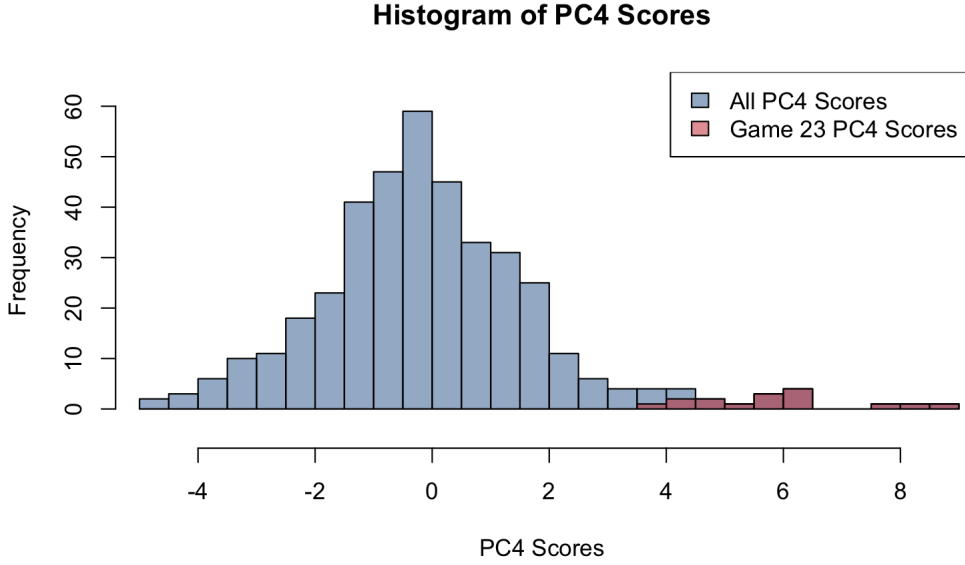


Figure 7: Histogram comparing the distribution of PC4 scores for all data (blue) versus Game 23 (red). The Game 23 PC4 scores are concentrated at higher values, suggesting this game had a larger amount of time spent in these low velocity and high acceleration quantiles.

3.3 Dirichlet-multinomial Regression

For our observed count matrix \mathbf{Y} , we assumed that each observation (row) $\mathbf{y}_i = (y_{i1}, y_{i2}, \dots, y_{id})$ follows a Dirichlet-multinomial distribution, which accounts for overdispersion and dependencies between quantiles. The Dirichlet-multinomial distribution is given by:

$$f_{DM}(\mathbf{y}_i|\boldsymbol{\alpha}) = \int_{\boldsymbol{\pi}} f_M(\mathbf{y}_i|N_i, \boldsymbol{\pi}) f_D(\boldsymbol{\pi}|\boldsymbol{\alpha}) d\boldsymbol{\pi} = \frac{\Gamma(N_i + 1) \Gamma(\sum_{j=1}^d \alpha_j)}{\Gamma(N_i + \sum_{j=1}^d \alpha_j) \prod_{j=1}^d \frac{\Gamma(y_{ij} + \alpha_j)}{\Gamma(\alpha_j) \Gamma(y_{ij} + 1)}}. \quad (1)$$

where $\boldsymbol{\alpha} = (\alpha_1, \alpha_2, \dots, \alpha_d)$ are positive concentration parameters and $N_i = \sum_{j=1}^d y_{ij}$ is the total count for observation i (Mosimann, 1962; Chen and Li, 2013).

We adopted the Dirichlet-multinomial distribution over a simple multinomial distribution for several key reasons. Since the Dirichlet-multinomial is a Dirichlet-mixture of multinomial distributions, it accounts for overdispersion, as the multinomial model assumes that the variance of category counts is determined solely by the total count and category probabilities. In real-world movement data, additional variability arises due

to differences across individuals, match conditions, and other external factors. Second, it accommodates compositional dependence among quantiles; movement intensities are not independent, as time spent in one quantile necessarily affects time spent in others. The Dirichlet-multinomial naturally models this structured dependence. Third, it allows for heterogeneity across athletes, whose movement patterns vary based on position, fitness level, and playing style. The Dirichlet prior introduces individual-level variation in category counts, enabling the model to reflect these differences. Finally, it captures the clustered nature of movement activity, where periods of high-intensity movement are followed by recovery phases, leading to non-uniform distributions of quantile counts. The Dirichlet-multinomial’s flexible variance structure enables it to model such clustering more effectively than a standard multinomial approach.

While this distribution addresses overdispersion and dependencies between quantiles, it does not incorporate external covariates that influence movement patterns. To extend the model’s applicability, we implemented a Dirichlet-multinomial regression framework, where $\boldsymbol{\alpha}$ is parameterized as a function of relevant covariates. This approach extends traditional multinomial regression by imposing additional structure on the probabilities through the Dirichlet distribution, making it particularly suited for modeling categorical outcomes with inherent dependencies while accounting for individual and contextual variations in movement behavior (Mosimann, 1962; Chen and Li, 2013).

We have the observed count matrix $\mathbf{Y} = (y_{ij})_{n \times d}$, and design matrix $\mathbf{X} = (x_{ik})_{n \times p}$ of $p = 13$ covariates. The Dirichlet-multinomial parameters α_j for $j = 1, \dots, d$ are modeled using the log-linear form:

$$\alpha_j = \eta(\mathbf{x}_i) := \exp(\beta_{j0} + \sum_{k=1}^p \beta_{jk} x_{ik}), \quad (2)$$

where β_{j0} is a constant for each j and β_{jk} is the coefficient for the j^{th} dimension with respect to the k^{th} covariate (Mosimann, 1962; Chen and Li, 2013). We evaluated several regression models to evaluate the relationships between the quantile cube distributions and various covariates, including match characteristics and athlete-specific factors. Our

analysis identified the optimal model specification to include half (1st and 2nd), position group (defender, midfielder, and forward), and mean-centered log(playing time) as covariates, where positive values of the standardized playing time indicate above-average duration and negative values indicate below-average duration.

Figures 8 and 9 show the coefficients for each of the covariates for the Dirichlet-multinomial regression model (DMM), including significance. The coefficients were deemed significant if $\left| \frac{\beta_{jk}}{SE_{\beta_{jk}}} \right| > 3$ where β_{jk} is the coefficient for the j^{th} dimension with respect to the k^{th} covariate from Equation (2) and the cutoff of three is chosen based on the distribution of our dataset.

From the significant coefficient values obtained in the analysis, we observe distinct trends in athlete movement patterns in relation with time. On the left of Figure 8, we see that during the second half, athletes tend to spend less time in the higher quantiles of velocity across all quantiles of acceleration and angle compared to the first half. On the right of Figure 8, it is evident that athletes with above-average playing time per half spend significantly less time in the lower quantiles of both velocity and acceleration, particularly in quantile one moving forward and backward.

When examining differences by playing position (Figure 9), defenders, midfielders, and forwards exhibit distinctive movement profiles. Compared to defenders, midfielders spend more time in the lower quantiles of both velocity and acceleration, as well as in the highest quantile of velocity across all levels of acceleration. Forwards, on the other hand, generally spend less time in the middle and lowest velocity quantiles across acceleration quantiles, except for the first velocity quantile in the highest acceleration quantile, compared to defenders. We also note that forwards spend significantly less time moving left to right than moving forward and backward, compared to defenders.

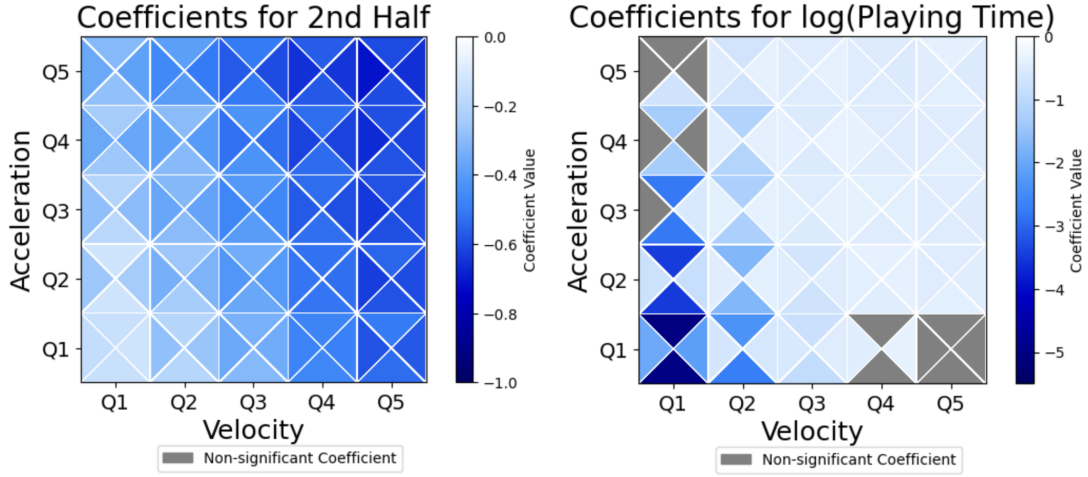


Figure 8: Quantile cube illustrating the DMM coefficients for the second half (left) and $\log(\text{Playing Time})$ (right). Non-significant coefficients are shown in gray, while significant coefficients are color-coded based on effect size, with intensity indicating magnitude.

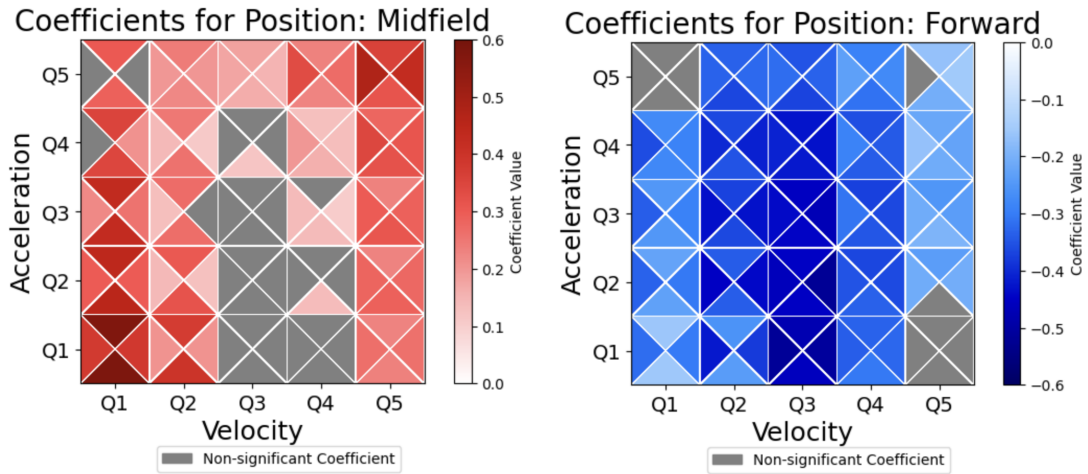


Figure 9: Quantile cube depicting the DMM coefficients for player position, where the defender is treated as the base class. Coefficients for comparisons with midfielders are shown on the left, and those for forwards are shown on the right. Non-significant coefficients are shaded in gray, while significant coefficients are color-coded based on effect size and direction: blue for negative effects and red for positive effects, with intensity reflecting magnitude.

4 Discussion

This paper presents a novel adaptation of established methodologies for assessing external load in elite female soccer athletes, with a focus on improving the interpretability of movement patterns during match play. By leveraging wearable GPS data, we examined the relationships between velocity, acceleration, and angle of movement with athlete and

game characteristics. Our findings offer insights that could potentially be applied in the future to optimize training and to enhance injury prevention strategies for elite athletes.

Our analysis revealed significant differences in athlete movement patterns between the first and second halves of matches. Consistent with previous research - such as that by Barrera et al. (2021), which found reductions in external load metrics such as high-speed running during the second half for male professional Portuguese soccer players - our results indicate time influences movement dynamics. Specifically, the quantile cube distribution of movements in the first and second halves exhibits statistically significant differences in their underlying distributions, reinforcing the idea that athlete performance and movement patterns evolve as the match progresses.

Additionally, the use of Principal Component Analysis (PCA) to reduce the dimensionality of the quantile cubes revealed several distinct periods of time with differing patterns of movement. This approach not only simplified the complexity of the data but also enhanced the interpretability of variations in movement patterns. Specifically, significant deviations in movement patterns were identified during the second half of match 1 and throughout match 23 compared to other matches over the course of the season. These deviations may indicate underlying changes in player dynamics, strategic adjustments, or external factors, such as varying match contexts or states of the season, that influence performance during these periods.

The Dirichlet-multinomial model (DMM) further allowed us to evaluate the relationships between the quantile cube distributions and various covariates. This model further confirmed the difference in movements between the first and second halves. Notably, the analysis revealed that during the second half, athletes tend to spend less time in the higher quantiles of both velocity and acceleration, suggesting a decline in intensity as the game progresses, likely due to fatigue or change in game strategy. This is consistent with Barrera et al.'s (2021) findings. Additionally, the model highlighted that athletes with high playing time per half spend less time in the lower quantiles of both velocity and acceleration, particularly in quantile one. This suggests athletes with high playing time may maintain a higher baseline level of workload throughout the game.

The coefficients of the DMM also revealed notable differences based on position. Midfielders displayed a distinctive movement profile, spending more time in both the lowest and highest quantiles of velocity and acceleration and in the highest quantile of velocity across all levels of acceleration compared to defenders. This suggests that midfielders experience a broader range of movement demands compared to defenders, ranging from low-intensity activities to high-speed bursts, reflecting their dynamic role on the field. In line with these findings, Wehbe et al. (2014) observed that male professional midfielders covered significantly more total distance (11.69%) and high-intensity running (28.08%) compared to defenders. They also reported that midfielders had a 10.93% higher average speed than defenders. While Wehbe et al.'s (2014) study focused on male athletes, these findings support the idea that midfielders engage in a wider variety of movement intensities throughout a match, as further evidenced by our analysis.

Forwards, on the other hand, spent significantly less time in the middle velocity quantiles across all levels of acceleration compared to defenders, particularly with left and right movements. This suggests that they alternate between periods of low activity and peak speed in the forward and backward directions - a pattern that aligns with their primary offensive, goal-oriented responsibilities requiring quick sprints towards goal, followed by recovery periods tracking back. However, Wehbe et al. (2014) found that male forwards performed significantly fewer medium accelerations than defenders, indicating that movement demands may vary by gender, game level, or tactical strategy. Their research also revealed that defenders, despite covering lower total and high-intensity running distances, face relatively high acceleration demands, challenging assumptions that their match load is lower (Wehbe et al., 2014). This underscores the importance of considering velocity and acceleration metrics, rather than just overall distance, when analyzing athlete movement profiles.

Our work introduces an accessible statistical method that transforms raw GPS measurements into probabilistic insights about athlete movement patterns. The Dirichlet-multinomial model's structure allows for the seamless integration of additional covariates, enabling robust analysis of how various factors influence athletes' movements. By quanti-

ifying the probability of specific movement patterns given athlete and match characteristics, we provide a novel framework for understanding player behavior. This probabilistic approach allows sports scientists to test hypotheses about movement modifications under different conditions and estimate the magnitude of these effects.

The model's extensible nature means new variables can be incorporated to examine their relationship with movement patterns - from environmental conditions to tactical changes. For instance, the probability of high-intensity movements can be modeled as a function of not just position or game context, but also of athlete physiological characteristics, weather conditions, or even opponent characteristics. Specifically, one could examine how factors such as soreness and sleep duration in the days leading up to a match influence the likelihood of certain movements for individual athletes. This statistical framework supports both inference about current patterns and prediction of future movements, enabling evidence-based decisions about training load and recovery protocols.

Furthermore, real-time implementation of this methodology could enhance in-game decision making through probabilistic analysis of movement patterns. When integrated with continuous GPS data streams from both training and matches, the model can establish player-specific baseline distributions and detect statistically significant deviations, distinguishing meaningful changes from random variation. This transforms continuous GPS monitoring from simple tracking into a robust statistical tool, where decisions about player management are grounded in probability theory and statistical inference rather than arbitrary thresholds. The ability to quantify the likelihood of movement pattern changes in real-time provides a more rigorous approach to identifying potential fatigue or injury risks, while controlling for false positives through proper statistical testing.

This study offers several key strengths that contribute to its novelty and utility in the sports analytics field. The use of a quantile cube to segment the GPS data into identifiable components, combined with the Hellinger Distance metric, Principal Component Analysis (PCA), and Dirichlet-multinomial regression, introduces an innovative framework for analyzing and interpreting complex movement patterns. Though a multinomial model could typically be applied in this setting, our framework captures the nuances

of athlete movements in a more personalized and comprehensive manner compared to traditional methods. Moreover, the use of wearable GPS devices ensures high precision in tracking real-time movements, providing a robust dataset that reduces subjectivity. By deconstructing the raw GPS data into identifiable movement components, we can see how specific components of athlete movement patterns evolve over the course of a match or training session. The quantile cube approach, paired with the Dirichlet-multinomial distribution, enables both the visualization of changes and the identification of differences in distributions. Additionally, the integration of a Dirichlet-multinomial regression model with covariates such as match and player attributes offers an interpretable framework for predicting the probability of specific movements.

Furthermore, our female-specific dataset innately offers a different perspective to existing research in this space. As much of the existing literature focuses on male athletes, this study fills a critical gap by shedding light on movement dynamics in elite female soccer athletes.

Despite these strengths, the study also has limitations that warrant consideration. Firstly, the analysis was limited to nine athletes with 23 match sessions, which, while providing valuable insights, may not fully capture variability across larger populations or diverse competitive environments. Our analysis did not include goalkeepers and did not separate wide and central midfielders nor wide and central defenders into separate categories due to the small sample size. Taking into account these positions as separate categories may reveal additional differences in movement patterns as studies have found that in male soccer athletes, wide position players typically produce higher acceleration efforts than central position players (Ingebrigtsen et al., 2015).

Additionally, our study did not account for training sessions or internal load factors, which could provide valuable context for understanding movement patterns on match day. The analysis also does not consider external variables such as weather conditions, pitch quality, or opposition strength, which could influence movement dynamics. Future studies could incorporate these factors to provide a more comprehensive analysis.

A final limitation is that although wearable GPS devices are highly effective, they may

have restrictions in accurately capturing certain movements, particularly abrupt changes in direction or movement under physical duress (e.g., during tackles). On the other hand, advances in technology have led to devices that capture additional real-time metrics, such as heart rate, which could be valuable additions to this analysis. By addressing these limitations in future research, the field can advance toward more robust and actionable models for optimizing athlete workload, performance, and well-being.

In summary, this study illustrates the statistical advantages of employing the “quantile cube” methodology to analyze external load in elite female soccer athletes, offering significant insights through these advanced analytical techniques. By identifying key movement patterns and quantifying their relationships with athlete and match characteristics, this work lays the foundation for the development of data-driven interventions aimed at optimizing athlete performance and mitigating injury risk. Future research should focus on examining longitudinal trends and integrating additional covariates to refine these statistical models, enhancing their generalizability and applicability across varied athletic populations.

References

- Bai, Z. and Saranadasa, H. (1996), ‘Effect of high dimension: By an example of a two-sample problem’, *Statistica Sinica* **6**, 311–329.
- Barrera, J., Sarmiento, H., Clemente, F. M., Field, A. and Figueiredo, A. J. (2021), ‘The effect of contextual variables on match performance across different playing positions in professional portuguese soccer players’, *International Journal of Environmental Research and Public Health* **18**, 5175.
- Bourdon, P. C., Cardinale, M., Murray, A., Gastin, P., Kellmann, M., Varley, M. C., Gabbett, T. J., Coutts, A. J., Burgess, D. J., Gregson, W. and Cable, N. T. (2017), ‘Monitoring athlete training loads: Consensus statement’, *International Journal of Sports Physiology and Performance* **12**(Suppl 2), S2161–S2170.

- Casella, G. and Berger, R. L. (2002), *Statistical Inference*, Thomson Learning Inc. Citing Chapters 8 and 11.
- Chen, J. and Li, H. (2013), ‘Variable selection for sparse dirichlet-multinomial regression with an application to microbiome data analysis’, *The Annals of Applied Statistics* **7**(1).
- Chen, S. X. and Qin, Y.-L. (2010), ‘A two-sample test for high-dimensional data with applications to gene-set testing’, *The Annals of Statistics* **38**(2), 808–835.
- Cummins, C., Orr, R., O’Connor, H. and West, C. (2013), ‘Global positioning systems (gps) and microtechnology sensors in team sports: A systematic review’, *Sports Medicine* **43**(10), 1025–1042.
- Ferraz, A., Duarte-Mendes, P., Sarmiento, H., Valente-Dos-Santos, J. and Travassos, B. (2023), ‘Tracking devices and physical performance analysis in team sports: a comprehensive framework for research—trends and future directions’, *Frontiers in Sports and Active Living* **5**.
- Google Maps API (2025), ‘Google maps platform documentation’, <https://developers.google.com/maps/documentation>. [Accessed: January 14, 2025].
- Ingebrigtsen, J., Dalen, T., Hjelde, G. H., Drust, B. and Wisløff, U. (2015), ‘Acceleration and sprint profiles of a professional elite football team in match play’, *European Journal of Sport Science* **15**(2), 101–110.
- Jolliffe, I. T. (2002), *Principal Component Analysis*, Springer.
- Luo, L. and Song, P. X.-K. (2020), ‘Renewable estimation and incremental inference in generalized linear models with streaming data sets’, *Journal of the Royal Statistical Society Series B: Statistical Methodology* **82**(1), 69–97.
- Luo, L. and Song, P. X.-K. (2023), ‘Multivariate online regression analysis with heterogeneous streaming data’, *Canadian Journal of Statistics* **51**(1), 111–133.

- Luo, L., Wang, J. and Hector, E. C. (2023), ‘Statistical inference for streamed longitudinal data’, *Biometrika* **110**(4), 841–858.
- Mosimann, J. E. (1962), ‘On the compound multinomial distribution, the multivariate β distribution, and correlations among proportions’, *Biometrika* **49**(1/2), 65–82. Publisher: [Oxford University Press, Biometrika Trust].
- Pebesma, E. (2018), ‘Simple features for r: Standardized support for spatial vector data’, *The R Journal* **10**(1), 439–446.
- Rossi, A., Pappalardo, L., Cintia, P., Iaia, F. M., Fernández, J. and Medina, D. (2018), ‘Effective injury forecasting in soccer with GPS training data and machine learning’, *PLOS ONE* **13**(7).
- Vaart, A. W. V. D. (1998), *Asymptotic Statistics*, 1 edn, Cambridge University Press.
URL: <https://www.cambridge.org/core/product/identifier/9780511802256/type/book>
- Vallance, E., Sutton-Charani, N., Imoussaten, A., Montmain, J. and Perrey, S. (2020), ‘Combining Internal- and External-Training-Loads to Predict Non-Contact Injuries in Soccer’, *Applied Sciences* **10**(15).
- Wehbe, G. M., Hartwig, T. B. and Duncan, C. S. (2014), ‘Movement analysis of australian national league soccer players using global positioning system technology’, *Journal of Strength and Conditioning Research* **28**(3), 834–842.

Acknowledgements

We extend our gratitude to Elena Cantu, Sam Moore, and Dr. Abbie Smith-Ryan from the Applied Physiology Lab in the University of North Carolina at Chapel Hill’s Department of Exercise and Sport Science for their generous contributions in gathering and providing access to the data.

Funding

Jan Hannig's research was supported in part by the National Science Foundation under Grant No. DMS-1916115, 2113404, and 2210337.